

Charge carrier mobility and lifetime versus composition of conjugated polymer/fullerene bulk-heterojunction solar cells

G. Dennler^{a,*}, A.J. Mozer^b, G. Juška^c, A. Pivrikas^d, R. Österbacka^d,
A. Fuchsbauer^a, N.S. Sariciftci^a

^a Linz Institute for Organic Solar Cells (LIOS), Johannes Kepler University Linz, Altenbergerstrasse 69, A-4040 Linz, Austria

^b Molecular Process Engineering, Graduate School of Engineering, Osaka University, Japan

^c Department of Solid State Electronics, Vilnius University, Lithuania

^d Department of Physics, Åbo Akademi University, Turku, Finland

Received 22 December 2005; received in revised form 27 February 2006; accepted 28 February 2006

Available online 18 April 2006

Abstract

Charge carrier mobility (μ), recombination kinetics, and lifetime (τ) have been investigated with the photo-induced charge carrier extraction by linearly increasing voltage technique (photo-CELIV) in blends of poly[2-methoxy-5-(3,7-dimethylthioctyloxy)-phenylene vinylene] (MDMO-PPV) and 1-(3-methoxycarbonyl)propyl-1-phenyl-(6,6)-C₆₁(PCBM). Different MDMO-PPV/PCBM ratios have been studied showing that increasing the PCBM content induces an increase of the photo-CELIV mobility up to two orders of magnitude. Simultaneously, the lifetime of the charge carriers decreases in such a way that the product $\mu \times \tau$ appears almost constant independently of the blend composition. Recombination kinetics close to the Langevin one is observed for all PCBM concentrations studied.

© 2006 Elsevier B.V. All rights reserved.

PACS: 72.20.Jv; 72.80.Le; 73.50.Pz

Keywords: Mobility; Recombination kinetics; Lifetime; Bulk-heterojunction; Conjugated polymer; Fullerene; Organic solar cells

1. Introduction

During the last five years, important research efforts have been devoted to acquire a better understanding of the working principle of conjugated polymer:fullerene based bulk-heterojunction solar

cells [1]. This knowledge sounds mandatory to allow further optimization and potential increase of the efficiency of these devices [2]. It appeared quickly that the ratio donor/acceptor does dictate not only the number of charge carriers created per incoming photons [3], but as well the ability of the device to collect the photo-induced charge carriers, that is, the transport properties of the active blend [4].

Several previous works focused on the investigation of solar cells characteristics versus conjugated

* Corresponding author. Tel.: +43 732 2468 1213; fax: +43 732 2468 8770.

E-mail address: gilles.dennler@jku.at (G. Dennler).

polymer/fullerene ratio [4–9]. In the case of poly [2-methoxy-5-(3,7-dimethyloctyloxy)-phenylenevinylene] (MDMO-PPV):1-(3-methoxycarbonyl)propyl-1-phenyl-(6,6)-C₆₁(PCBM) blends, short circuit current (I_{sc}), fill factor (FF) and overall efficiency (η) were reported to show optimum values for PCBM concentration about 80% [7,9]. These results have been interpreted in terms of competing effects between charge generation, taking essentially place in the MDMO-PPV molecules, and hole and electron respective mobilities. These latter have both been reported to increase up to two orders of magnitude upon increasing the PCBM concentration [9,10]. Among others, ordering effects have been invoked to explain this unexpected phenomenon. This hypothesis has been substantiated by the numerous morphology studies performed on MDMO-PPV:PCBM, which show that PCBM tends to form nano-clusters due to its quite high diffusion coefficient in amorphous MDMO-PPV [7,8]. This nano-clusters have been proposed to enhance the organization of the long MDMO-PPV chains, and hence the hole mobility [11].

In several models proposed to describe the working principle of conjugated polymer:fullerene solar cells, the charge collection is considered to be mostly ensured by field driven drift, yet diffusion might play a non-negligible role, especially close to the electrodes [9,12,13]. In this perspective, the distance performed by the charge carriers is given by

$$l = \mu \cdot \tau \cdot E, \quad (1)$$

where μ is the mobility of the charge carriers, τ their lifetime, and E the electric field in the device. Thus, the mobility indeed plays a major role in the collection of charge carriers. But so does as well the charge carrier lifetime. To the best of our knowledge, no one did yet report the evolution of τ versus the concentration of the MDMO-PPV:PCBM blend. Mihailitchi et al. expressed the necessity of their model to suppose increasing τ with decreasing PCBM to fit properly the experiment data, especially in the range below 50% of PCBM [9]. But no direct evaluation of τ was performed. Nevertheless, it has to be mentioned that Montanari et al. studied the recombination kinetic of charge carriers by transient absorption spectroscopy (TAS) [14]. However, the authors reported a PCBM concentration independent recombination kinetics as detected with this optical method.

Thus, we have used photo-induced charge carrier extraction by linearly increasing voltage technique

(photo-CELIV) to investigate the charge carrier mobility, recombination kinetic and lifetime.

2. Experimental

As described in details elsewhere [15–17], photo-CELIV is a powerful method that allows the determination of charge carrier transport properties in the μ s to ms range: a short laser pulse (3 ns, 532 nm, 0.5 mJ/pulse, Nd-YAG laser in our case) is absorbed by the device to be characterized; the charge carriers created are forced to recombine in the device thanks to an offset bias applied to compensate the Voc of the solar cell, what ensures flat-band condition; after a certain delay time τ_{del} , the remaining charges are extracted by a linearly increasing voltage $A = dU/dt$ applied in the reverse, non-injecting polarization of the photodiode. The devices studied in this work are MDMO-PPV:PCBM bulk-heterojunctions solar cells with PCBM concentrations varying from 0% to 80% (in weight, in the entire text). The chlorobenzene based solutions have been spin-cast on indium tin oxide (ITO), and coated with evaporated aluminum (Al, 70 nm) after drying in vacuum. The thickness of the device is comprised between 150 and 250 nm and the active surface area between 4 and 6 mm². All the photo-CELIV measurements have been carried out under high vacuum (10⁻⁶ mbar) at room temperature.

3. Results and discussion

Fig. 1a shows the photo-CELIV curves collected in the case of a 30% MDMO-PPV:70% PCBM active layer for various τ_{del} . One can observe a capacitance induced displacement current to which is superimposed an extraction current [15–17]. This latter disappears after 8 μ s, indicating a complete extraction of the charge carrier photogenerated. The mobility of the carriers can be calculated according to Eq. (2):

$$\mu = \frac{2 \cdot d^2}{3 \cdot A \cdot t_{max}^2 \left[1 + 0.36 \frac{\Delta j}{j(0)} \right]} \quad \text{if } \Delta j \leq j(0) \quad (2)$$

where d is the thickness of the device, A is the voltage rise speed, t_{max} is the time at the maximum Δj of the extraction peak, and $j(0)$ is the displacement current of the capacitance. Using Eq. (2), we find a mobility $\mu = 1.9 \times 10^{-4} \text{ cm}^2 \text{ V}^{-1} \text{ s}^{-1}$. Moreover, it can be noted that the number of extracted charge

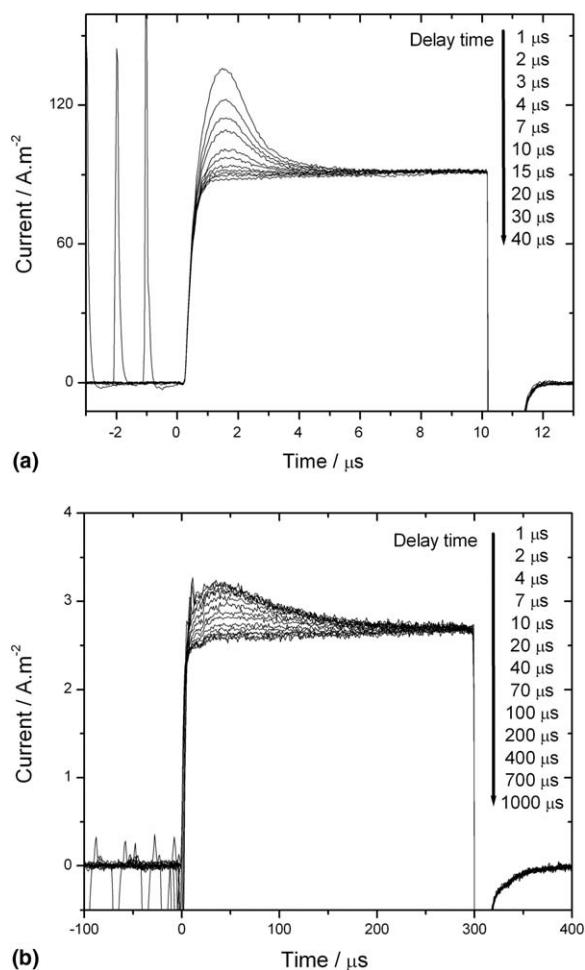


Fig. 1. Photo-CELIV curves for various delay times between the light pulse and the extraction voltage ramp in the case of (a) a 30% MDMO-PPV:70% PCBM blend ($A = 5 \text{ V}/10 \mu\text{s}$, $d = 155 \text{ nm}$) and (b) a 70% MDMO-PPV:30% PCBM blend ($A = 5 \text{ V}/300 \mu\text{s}$, $d = 200 \text{ nm}$).

carriers, that is the area under the extraction peak, decreases with increasing delay time between the light pulse and the beginning of the extraction. This indicates that a recombination process takes place during τ_{del} , while flat-band condition is ensured in the device thanks to the applied offset voltage.

Fig. 1b exhibits the photo-CELIV transients collected in the case of a 70% MDMO-PPV:30% PCBM active layer for various τ_{del} . Although the curves show qualitatively the same behavior than in Fig. 1a, a quantitative analysis suggests major differences. The application of Eq. (2) reveals that the mobility of the charge carriers drastically decreases with decreasing PCBM concentration: μ is found to be about $1 \times 10^{-5} \text{ cm}^2 \text{ V}^{-1} \text{ s}^{-1}$. More-

over, long lived charges can still be extracted after several hundreds of μs after the light pulse, what suggests that the lifetime of the charges is considerably enhanced compared to the situation displayed in Fig. 1a, where all the carriers recombine within less than $100 \mu\text{s}$. Finally, a close observation reveals that the shape of the photo-CELIV peak changes from Fig. 1a and b. This shape can be numerically analyzed by calculating the ratio $t_{1/2}/t_{\text{max}}$, where t_{max} is the time at the maximum of the peak, and $t_{1/2}$ is the width at half maximum of the extraction peak [18]. In the case of ideal non-dispersive transients $t_{1/2}/t_{\text{max}} = 1.2$, and this ratio increases with increasing dispersivity. The value extracted for Fig. 1a and b are 1.2 and 2.4, respectively. This shows that the dispersive character of the transient decreases with increasing PCBM concentration, as observed by Pacios et al. in the case polyfluorene:PCBM blends [19].

A more detailed investigation of the charge carrier mobility and decay versus blend composition has been performed. Fig. 2 exhibits the time dependence of the charge carrier mobility and the number of charge carriers extracted. As a first observation, one can note that, as mentioned above and reported previously by several groups [9,10], the charge carrier mobility increases with increasing PCBM concentration, from $3 \times 10^{-6} \text{ cm}^2 \text{ V}^{-1} \text{ s}^{-1}$ for the pure MDMO-PPV to about $3 \times 10^{-4} \text{ cm}^2 \text{ V}^{-1} \text{ s}^{-1}$ for the 1:4 ratio (at $\tau_{\text{del}} = 1 \mu\text{s}$). Though the sign of the charge carriers investigated with photo-CELIV remains under debate, these values are believed to be related to the slowest carriers [20], namely the holes. These values are in close accordance to the hole mobilities reported by Mihailetschi et al. [9]. Moreover, Fig. 2a indicates a slightly time dependent mobility for almost all PCBM concentrations studied. This phenomenon, already reported elsewhere for 20% MDMO-PPV: 80% PCBM solar cell, has been attributed to energy relaxation of the charge carriers towards the tail states of the density of states (DOS) distribution [20].

Fig. 2b shows the number of charge carriers extracted versus the delay time between light pulse and extraction. As illustrated in Fig. 1, $n(t)$ drastically decreases with increasing time since the charge carriers are forced to recombine in the device. The saturation of the number of carriers extracted versus light intensity (not shown here), observed for all PCBM concentration suggests that the recombination kinetic is of bimolecular nature in the regime studied. This bimolecular regime has been proposed

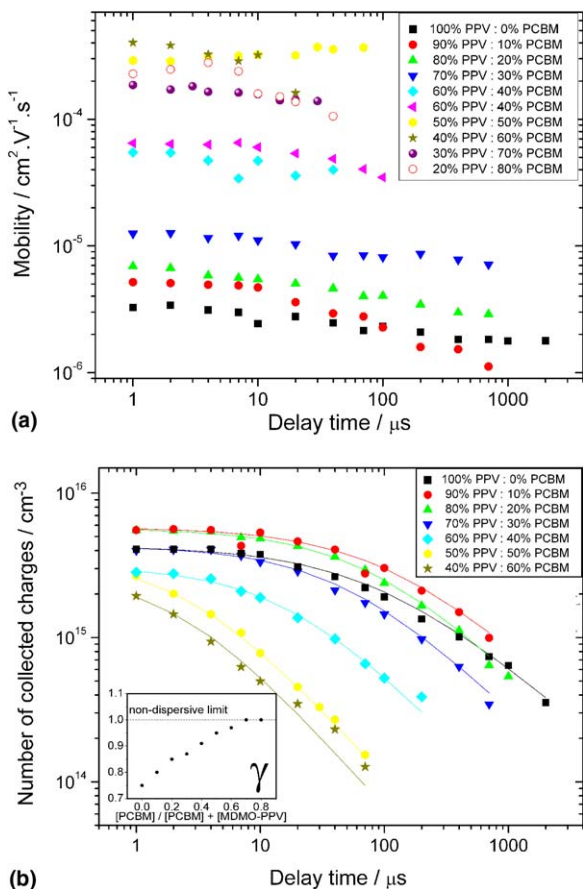


Fig. 2. (a) Photo-CELIV mobility and (b) number of extracted charge carriers versus delay time measured for different MDMO-PPV:PCBM ratios. In (b), the solid lines are fits realized using Eq. (5). The inset in (b) shows the evolution of γ versus the composition of the blend.

to be of primary importance in the recombination kinetics in solar cells in operation [21], especially in situations close to the open circuit condition.

Moreover, Fig. 2b shows that for low PCBM concentrations, the lifetime of the charge carriers is much longer than for high PCBM concentrations. In order to extract the value of the charge carriers bimolecular lifetime, the $n(t)$ data have been fitted with a dispersive bimolecular recombination dynamics model [20]: The observation of a time dependent mobility during thermalization suggests a time dependent bimolecular recombination rate

$$\frac{dn}{dt} = \frac{dp}{dt} = -\beta(t) \cdot n \cdot p, \quad (3)$$

where n and p are the concentration of electrons and hole, respectively, and $\beta(t)$ the time dependent bimolecular recombination coefficient.

Assuming charge neutrality, and using the following functional form of $\beta(t)$

$$\beta(t) = \beta_0 \cdot t^{-(1-\gamma)}, \quad (4)$$

where β_0 and γ are time independent parameters, Eq. (5) can be yielded:

$$n(t) = p(t) = \frac{n(0)}{1 + (t/\tau_B)^\gamma}. \quad (5)$$

τ_B , called the “effective” bimolecular lifetime, can be expressed as follow:

$$\tau_B = \left(\frac{\gamma}{n(0) \cdot \beta_0} \right)^{\frac{1}{\gamma}} \quad (6)$$

The fits to the decay data, displayed as solid lines in Fig. 2b, show good agreement with the experimental data. The values of γ , extracted for each PCBM concentrations are found to evolves from 0.75 to 1 with increasing PCBM concentration, indicating a transition from a dispersive to a non-dispersive regime, as already noticed above. Finally μ and τ_B extracted for each concentration are shown in Fig. 3. While the mobility clearly increases by two orders of magnitude upon adding PCBM, the “effective” bimolecular lifetime decreases by the same factor, evolving from about 100 μ s to 2 μ s. Interestingly, these opposite evolutions induce a constant product $\mu \times \tau_B$ independent of the PCBM concentration, as revealed in the inset of Fig. 3.

It has been previously reported that the bimolecular recombination kinetics in PPV [22] and 20% MDMO-PPV:80% PCBM [20] is of Langevin type [23]. In this case, the Langevin bimolecular recombination coefficient β_L in given by

$$\beta_L(t) = B \cdot \mu(t) \quad \text{where } B = e/\varepsilon \cdot \varepsilon_0, \quad (7)$$

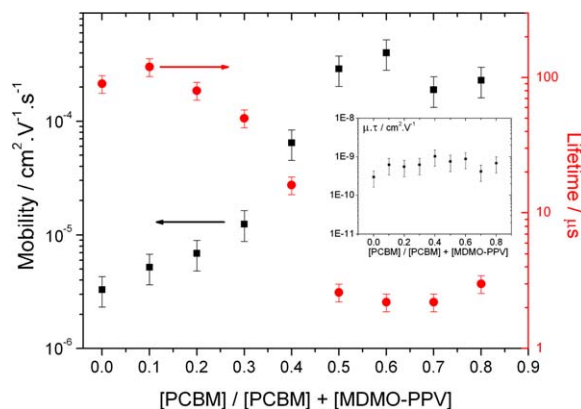


Fig. 3. Photo-CELIV mobility (μ) of charge carriers, “effective” bimolecular lifetime (τ_B) of charge carriers, and (inset) product $\mu \times \tau_B$ versus MDMO-PPV:PCBM ratio.

e being the elementary charge, ε the relative dielectric constant of the semiconductor (3 in our case), and ε_0 the permittivity of vacuum. In order to verify the nature of the bimolecular recombination kinetic observed in this study, we have fitted the $n(t)$ data of each PCBM concentration with Eq. (8). It should be noted here that while Eq. (6) (used to fit the data in Fig. 2b) supposes a bimolecular recombination kinetic (Eq. (3)) with a power law decay of the bimolecular recombination coefficient (Eq. (4)), Eq. (8) results from the supposition of a purely Langevin (Eq. (7)) bimolecular recombination kinetic (Eq. (3)):

$$n(t) = \frac{n(0)}{1 + n(0) \cdot B \cdot \int_0^t \mu(t) \cdot dt} \quad (8)$$

The results are exhibited in Fig. 4. It is visible that accurate fits are achieved for all PCBM concentrations with value of B comprised between 3 and 9×10^{-7} V cm that is very close to the theoretical value of $B = 6 \times 10^{-7}$ V cm. This allows us to conclude that in all cases investigated here, the nature of the bimolecular recombination kinetic is very close to being Langevin. This conclusion is consistent with the fact that the product $\mu \times \tau_B$ is constant for all PCBM concentrations. Indeed, surprisingly the $n(0)$ obtained by fitting the data in Fig. 2b are found to be all very close, comprised between 3 and 8×10^{15} cm $^{-3}$. Thus the variation of τ_B versus PCBM concentration appears to be directly related to the variation of the mobility (Eq. (7)), since $n(0)$ can be considered as almost constant.

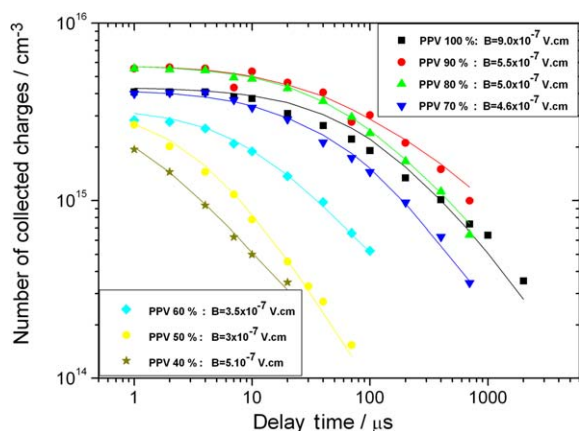


Fig. 4. Number of extracted charge carriers versus delay time measured for different MDMO-PPV:PCBM ratios and fitted with Eq. (8). The values of B used in the fits are indicated for each PCBM concentration. The values of the mobility used in Eq. (8) have been numerically integrated from Fig. 2a.

Finally, the intriguing point of the constancy of $n(0)$ versus PCBM concentration has to be addressed. As mentioned above, it is of common knowledge that the short circuit current of a MDMO-PPV:PCBM based solar cell is drastically dependent on the PCBM content in the blend. Contrarily to one's expectation, Fig. 2b shows that the number of charge carriers collected during photo-CELIV experiments does not obviously increase with PCBM concentration, but rather fluctuates within a factor 3. A rough estimation of the quantum efficiency yields values by orders of magnitude lower than that of a device in operation. This low efficiency might arise from the fact that the device is investigated in a bimolecular mode and that the light intensity used is important: according to Eq. (5), the number of extractable charges does saturate. Lower light intensities would yield higher quantum efficiencies. Moreover, Montanari et al. [14] have shown that charge carrier decay studied by TAS can be separated into two distinguished phases. The first one, ≤ 20 ns, is light intensity dependent while the second one, extending to the ms range was found to be light intensity independent above a certain threshold. This second decay regime exhibited a power law type behavior $OD \sim t^\alpha$, where OD is the optical density of the device at a certain wavelength, and α equals 0.4 in the case of MDMO-PPV:PCBM blends, independently of the PCBM concentration. This phenomenon was explained by diffusion controlled recombination kinetic combined with the presence of a mobility edge in the PPV derivative [24]: when the number of charge carriers photo-created exceeds the number of available localized states evaluated about 10^{17} cm $^{-3}$ in MDMO-PPV phase, charge carrier located above the MDMO-PPV mobility edge can diffuse faster, and therefore recombine faster (≤ 20 ns). Contrarily to TAS data, the transient decays measured by photo-CELIV do not follow a power law, and do depend on the PCBM concentration. Moreover, $n(0)$ was found to fluctuate around 5×10^{15} cm $^{-3}$, that is about 20 times less than the number of localized states available in MDMO-PPV, as proposed by Nelson. These differences might come from the different nature of the charge carriers probed by the two techniques: TAS is sensitive to optically active carriers, while photo-CELIV detects mobile charges able to contribute to an electrical current. However, the time scale investigated by photo-CELIV does correspond to the second decay phase described by Nelson [24] what might explain

why $n(0)$ does not vary with PCBM concentration. This leads us to the conclusion that, though photo-CELIV transients allow us to investigate the transport and recombination kinetics of long lived charges, it does not give access to the very fast (ns range) phenomena, which might be relevant for the understanding of the device operation.

4. Conclusion

In conclusion, we have studied the transient mobility, charge carrier recombination kinetic (in the μs range) and charge carrier lifetime in MDMO-PPV:PCBM blends by photo-CELIV. We have observed that the charge carrier mobility increases by two orders of magnitude with increasing PCBM concentration, while the “effective” bimolecular lifetime of charge carriers decreases drastically, as theoretically proposed by Mihailetchi et al. Hence, the product mobility \times lifetime of long lived charge carriers is found to be independent of the PCBM concentration. This effect is believed to be induced by Langevin type bimolecular recombination, found to control the recombination kinetics for all PCBM concentrations studied. Moreover, the dispersive character of the photo-CELIV transient and of the recombination kinetics is found to decrease with increasing PCBM concentration.

Acknowledgements

The authors gratefully acknowledge the financial support of the Austrian Foundation for the Advancement of Science (FWF NANORAC Contract No: FWF-N00103000). They thank H. Neugebauer and C. Lungenschmied for fruitful discussions.

References

- [1] C.J. Brabec, V. Dyakonov, J. Parisi, N.S. Sariciftci (Eds.), *Organic Photovoltaics: Concepts and Realization*, Springer, 2003.

- [2] C.J. Brabec, *Sol. Energy Mater. Sol. Cells* 83 (2004) 273.
 [3] H. Lee, G. Yu, D. Moses, K. Pakbaz, C. Zhang, N.S. Sariciftci, A.J. Heeger, F. Wudl, *Phys. Rev. B* 48 (1993) 15425.
 [4] G. Yu, J. Gao, J.C. Hummelen, F. Wudl, A.J. Heeger, *Science* 270 (1995) 1789.
 [5] J. Gao, F. Hide, H. Wang, *Synth. Met.* 84 (1997) 979.
 [6] D. Chirvase, J. Parisi, J.C. Hummelen, V. Dyakonov, *Nanotechnology* 15 (2004) 1317.
 [7] J.K.J. Van Duren, X. Yang, J. Loos, C.W.T. Bulle-Lieuwma, A.B. Sieval, J.C. Hummelen, R.A.J. Janssen, *Adv. Funct. Mater.* 14 (2004) 425.
 [8] H. Hoppe, M. Niggemann, C. Winder, J. Kraut, R. Hiesgen, A. Hinsch, D. Meissner, N.S. Sariciftci, *Adv. Funct. Mater.* 14 (2004) 1005.
 [9] V.D. Mihailetchi, L.J.A. Koster, P.W.M. Blom, C. Melzer, B. De Boer, J.K.J. Van Duren, R.A.J. Janssen, *Adv. Funct. Mater.* 15 (2005) 795.
 [10] W. Geens, T. Martens, J. Poortmans, T. Aernouts, J. Manca, L. Lutsen, P. Heremans, S. Borghs, R. Mertens, D. Vanderzande, *Thin Solid Films* 451–452 (2004) 498.
 [11] R. Pacios, D.D.C. Bradley, J. Nelson, C.J. Brabec, *Synth. Met.* 137 (2003) 1469.
 [12] P. Schilinsky, C. Waldauf, J. Hauch, C.J. Brabec, *J. Appl. Phys.* 95 (2004) 2816.
 [13] L.J.A. Koster, E.C.P. Smits, V.D. Mihailetchi, P.W.M. Blom, *Phys. Rev. B* 72 (2005) 085205.
 [14] I. Montanari, A.F. Nogueira, J. Nelson, J. Durrant, C. Winder, M.A. Loi, N.S. Sariciftci, C.J. Brabec, *Appl. Phys. Lett.* 81 (2002) 3001.
 [15] G. Juška, K. Arlauskas, M. Viliūnas, J. Kočka, *Phys. Rev. Lett.* 84 (2000) 4946.
 [16] R. Österbacka, A. Pivrikas, G. Juška, K. Genevicius, K. Arlauskas, H. Stubb, *Curr. Appl. Phys.* 4 (2004) 534.
 [17] A.J. Mozer, N.S. Sariciftci, L. Lutsen, D. Vanderzande, R. Österbacka, M. Westerling, G. Juška, *Appl. Phys. Lett.* 86 (2005) 112104.
 [18] G. Juska, N. Nekrasas, K. Genevicius, J. Stuchlik, J. Kocka, *Thin Solid Films* 451–452 (2004) 290.
 [19] R. Pacios, J. Nelson, D.D.C. Bradley, C.J. Brabec, *Appl. Phys. Lett.* 83 (2003) 4764.
 [20] A.J. Mozer, G. Denmler, N.S. Sariciftci, M. Westerling, A. Pivrikas, R. Österbacka, G. Juska, *Phys. Rev. B* 72 (2005) 035217.
 [21] H.H.P. Gommans, K. Kemerink, J.M. Kramer, R.A.J. Janssen, *Appl. Phys. Lett.* 87 (2005) 122104.
 [22] P.W.M. Blom, M.J.M. De Jong, S. Breedijk, *App. Phys. Lett.* 71 (1997) 930.
 [23] P. Langevin, *Ann. Chem. Phys.* 28 (1903) 289.
 [24] J. Nelson, *Phys. Rev. B* 67 (2003) 155209.